Available online at www.sciencedirect.com
ScienceDirect
Journal of Magnetism and Magnetic Materials 306 (2006) 218–222
www.elsevier.com/locate/jmmm

Dependence of magnetic properties on ferromagnetic layer thickness in trilayer Co/Ge/Co films with granular semiconducting spacer

G.S. Patrin[a,c,*], C.-G. Lee[b], I.A. Turpanov[a], S.M. Zharkov[a], D.A. Velikanov[a], V.K. Maltsev[a], L.A. Li[a], V.V. Lantsev[a]

[a]*L. V. Kirensky Institute of Physics, Siberian Branch of Russian Academy of Sciences, Krasnoyarsk, 660036, Russia*
[b]*Changwon National University, 9, Sarim-dong, Changwon, Gyeongnam, 641-773, Korea*
[c]*Krasnoyarsk State University, prospect Svobodnyi, 79, Krasnoyarsk, 660041, Russia*

Received 14 December 2005
Available online 30 March 2006

Abstract

We have investigated the magnetic properties of trilayer films of Co–Ge–Co. At a fixed thickness of germanium of 3.5 nm, the formation and distribution of metastable amorphous and cubic phases depends on the thickness of the ferromagnetic layer. The portion of the stable hexagonal phase is affected, too. Possible mechanisms for forming the observed magnetic structure are discussed.
© 2006 Elsevier B.V. All rights reserved.

PACS: 73.21.Ac; 75.70.Cn

Keywords: Trilayer film; Semiconducting spacer; Magnetization; Metastable magnetic phase

1. Introduction

The multilayer *ferromagnetic–semiconductor* films have been the object of much recent interest. In such films, a semiconducting, nonmagnetic layer is sandwiched between ferromagnetic ones. It has been seen that the outer layers can be coupled as a function of temperature [1], or the thicknesses of the spacer layer [2,3] and outer layers [4]. Unusual magneto-resistive properties have been observed [5]. Also the choice of semiconductor material can affect the magnetic and resistive properties of such system. If the nonmagnetic semiconducting interlayer is in a granular state, then novel materials for spintronics devices can be created [6].

2. Experimental

Co–Ge–Co films were prepared by the ion–plasma sputtering at a base pressure of 10^{-6} torr in an argon atmosphere. Glass was used as a substrate; the substrate temperature was 373 K during sputtering. To get semiconducting interlayer in a granular state, the deposition rates were selected to be, for cobalt, 0.15 nm/s and for germanium 0.12 ± 0.02 nm/s. Several films were made with a fixed germanium thickness of 3.5 ± 0.3 nm and varying cobalt layer thickness. The averaged layer thickness was determined by X-ray spectroscopy. The microstructure and phase composition of the film were determined using TEM (PREM-200). The structure of the cobalt phase was determined by two-pulse method of spin-echo NMR, with operating frequencies of 150–240 MHz. The high frequency probe pulse of magnetic field was 0.1–1.0 μs long at intervals of 4–5 μs.

The magnetization data were obtained by a SQUID-magnetometer operating in temperature range of 4.2–300 K and with magnetic fields up to 1 KOe in an in-plane geometry. Prior to each measurement, the films were placed into a demagnetizer and then cooled in zero magnetic field (ZFC regime).

3. Results

A TEM of the film with $t_{Co} = 10.5$ nm shows a microstructure of closely spaced spherical formations

*Corresponding author. L.V. Kirensky Institute of Physics, Siberian Branch of Russian Academy of Sciences, Krasnoyarsk, 660036, Russia.
E-mail addresses: patrin@iph.krasn.ru (G.S. Patrin), cglee@sarim.changwon.ac.kr (C.-G. Lee).

0304-8853/$ - see front matter © 2006 Elsevier B.V. All rights reserved.
doi:10.1016/j.jmmm.2006.02.259

about 0.5–1 μm against a background of fine particles with size less 10 nm. The diffraction parents show very broad polycrystalline rings. The selection area electron diffraction (SAED) data (see part 1(a) and (b) in Fig. 1 and the Table 1) suggest that the large spherical formations are mainly germanium with an α-Ge (Fd3 m) structure with lattice parameter $a = 0.56576$ nm (JCPDS card No.04-0545). The presence of a reflex with atomic interplanar spacing $d = 0.327$ nm corresponding to {1 1 1} planes of α-Ge is evidence of this. Also, other reflexes attributed to α–Ge phase are observed, but they practically coincide with the Co reflexes. On the diffraction patterns obtained from areas without big particles the reflex corresponding to $d = 0.327$ nm is not seen (see, part 2 in Fig. 1). Interpretation of the SAED leads us to conclude that the fine particles are (FCC)—Fm3 m cobalt with lattice parameter $a = 0.35447$ nm (JCPDS card no. 15-0806). An (HCP) cobalt phase, which would be indicated by an intense reflex

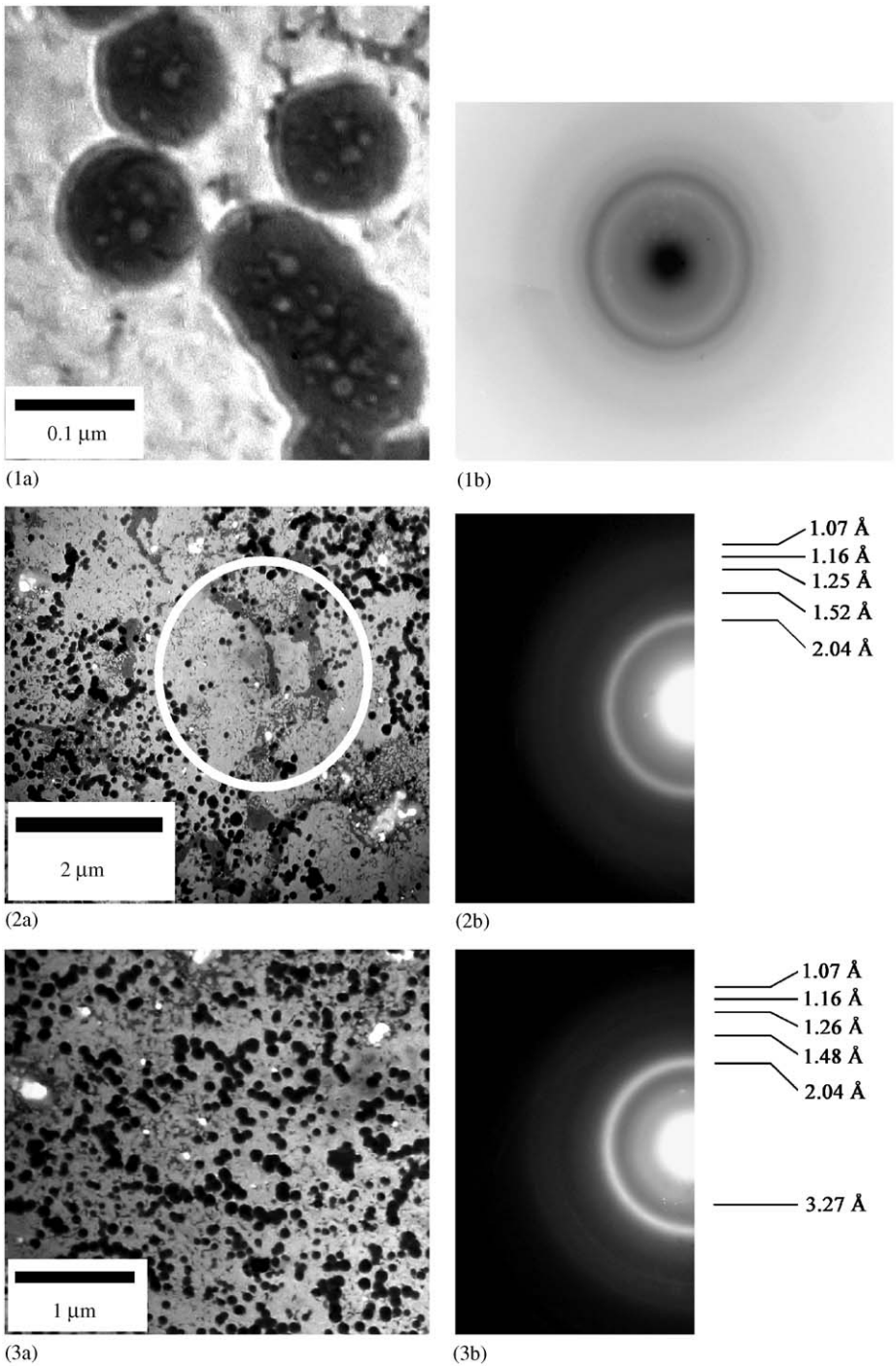

Fig. 1. Diffraction patterns of Co/Ge/Co films with $t_{Co} = 10.5$ nm, $t_{Ge} = 3.5$ nm. (a) Enlarged photo of the selected areas, (b) selection area electron diffraction. 1—germanium grains area, 2 and 3—cobalt areas without grains and with them, respectively.

Table 1
Structure decoding of Co/Ge/Co film (No.2)

Co/Ge/Co (SAED—1b) $C = 58.7$ (area with particles)			Co/Ge/Co (SAED—2b) $C = 58.7$ (area with particles)			Co/Ge/Co (SAED—3b) $C = 58.7$ (area with particles)			Co (JCPDS card no. 05-0727) $P6_3/mmc$ (194) $a = 2.5031$ Å, $c = 4.0605$ Å	Co (JCPDS card no. 15-0806) Fm3 m (225) $a = 3.5447$ Å	α–Ge (JCPDS card no. 04–0545) Fd3 m (227) $a = 5.6576$ Å		
D (mm)	*d* (Å)	*I* (rel.)	*D* (mm)	*d* (Å)	*I* (rel.)	*D* (mm)	*d* (Å)	*I* rel.	*d* (Å)–Int—*h k l*	*d* (Å)–Int—*h k l*	*d* (Å)	Int	*h k l*
18.0	3.27	Mean *halo*				18.0	3.27	Weak *halo*			3.266	100	111
22.9	2.56	Very weak							2.165–20–100				
28.9	2.03 ±0.06 + 0.3	Weak *halo*	28.8	2.04±0.15	Mean *halo*	28.7	2.04±0.08	very weak *halo*	2.023–60-002 1.91–100–101	2.047–100–111	2.00	57	2 2 0
33.7	1.74	mean								1.772–40–200	1.706	39	3 1 1
40.1	1.46	very weak	38.5	1.52	very very weak	39.6	1.48	very very weak	1.480–1–102		1.414	7	4 0 0
			46.9	1.25	weak	46.5	1.26	weak	1.252–80–110	1.253–25–220	1.298	10	3 3 1
			50.6	1.16	weak	50.6	1.16	weak	1.149–80–103		1.1547	17	4 2 2
52.9	1.11	weak							1.0835–20–200		1.0888	7	5 1 1
			54.9	1.07	weak	55.0	1.07	weak	1.066–80–112				
									1.047–60–201	1.069–30–311	1.000	3	4 4 0
									1.015–20–004	1.023–12–222	0.9562	11	5 3 1
											0.8946	6	6 2 0
											0.8628	4	5 3 3
											0.8166	2	4 4 4
											0.7923	8	5 5 1

D—ring diameter, *d*—interplane distance, *I* (Int.)—reflex intensity, rel.—relative, *h k l*—crystallographic indices.

corresponding to an interplanar spacing of $d_{101} = 0.191$ nm, is not observed. The center of the halo is in the area of the most intense reflex of the (FCC) phase, but there is no (HCP) phase visible. However, due to the large width of the halo and the displacement of its center one might still suppose that some (HCP) phase is present, but in much smaller quantities than (FCC).

The broadening in the diffraction reflexes shows that the coherence area within the germanium particles is not greater than 10 nm, meaning that some part of the germanium is in an amorphous state. There is no evidence of a Co–Ge phases. As seen in parts 2 and 3 of Fig. 1 the germanium does not cover entirely the film area entirely, but is rather uniformly distributed in grains in a cobalt background. The cobalt NMR spectrum is not a simple Lorenz curve (Fig. 2), but rather a superposition of two such curves, with one centered at $\omega_{1HF} = 213.26$ MHz, assigned to (FCC) phase and a second one at $\omega_{2HF} = 218.41$ MHz assigned to the (HCP) phase. The ratio of line intensities yields the relative proportion of each phase, here $(I_{FCC}:I_{HCP}) = (89:11)$, consistent with the TEM results. The film with $t_{Co} = 9 \pm 0.5$ nm (film 1) contains amorphous (AM) and cubic phases in ratio (76:24), and film 3, with $t_{Co} = 13.2 \pm 0.5$ nm, has amorphous, cubic and hexagonal phases in the ratio (13:52:35). The general trend is that an increase in the cobalt layer thickness rapidly lowers the amorphous phase fraction increases the hexagonal phase, while the cubic phase fraction stays relatively constant. When the cobalt layer thickness is decreased below $t_{Co} = 9$ nm, the amorphous phase becomes more probable, while the cubic phase is decreased. The cubic cobalt phase can disappear completely.

The magnetization dependence on temperature, $M(T)$, is shown in Fig. 3. It is seen that in low magnetic fields ($H = 50$ Oe) for films 1 and 3 show very similar $M(T)$. An abrupt rise in magnetization begins at about 200 K and continues to increase right up to room temperatures. The magnetization of film 2, however, begins to increase at the lowest temperatures tested, and levels off above 150 K. In stronger magnetic fields, the magnetization of film 2 is at saturation already at liquid helium temperatures, whereas films 1 and 3 reach saturation only at about 150 K.

The field dependence of the magnetization of these films at a constant temperature of 4.2 K is notably different, too (Fig. 4). Films 1 and 3 show a practically linear dependence, with only slight deviation from linearity for film 3 above 600 Oe. Film 2 shows typical behavior for a ferromagnetic system; saturation is achieved at 800 Oe.

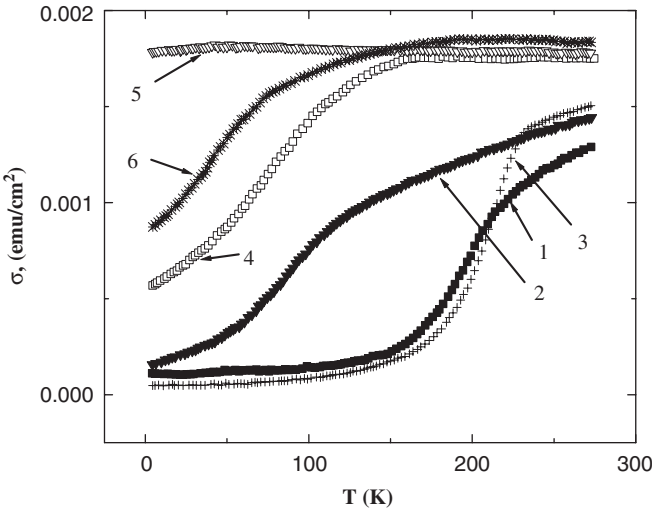

Fig. 3. Temperature dependences of the magnetic moments of a unit area in Co/Ge/Co films. Curves 1, 4–$t_{Co} = 9$ nm, curves 2, 5—$t_{Co} = 10.5$ nm, curves 3, 6—$t_{Co} = 13.2$ nm. Curves 1–3—$H = 50$ Oe, curves 4–6—$H = 800$ Oe.

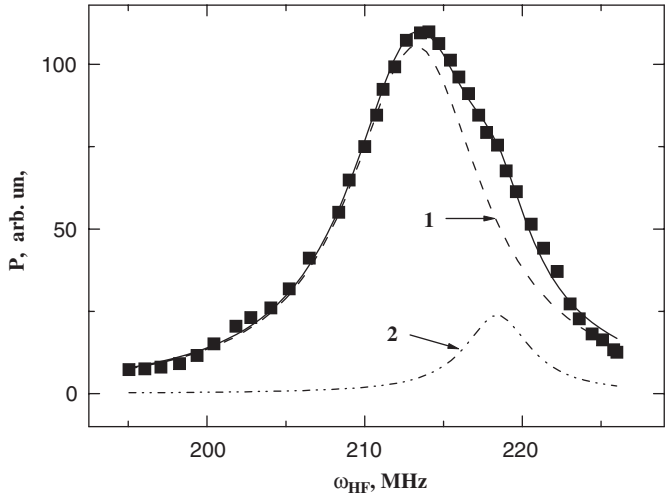

Fig. 2. NMR spectrum of Co/Ge/Co film with $t_{Co} = 10.5$ nm, $t_{Ge} = 3.5$ nm. 1—absorption line of the cubic phase, 2—absorption line of the hexagonal phase.

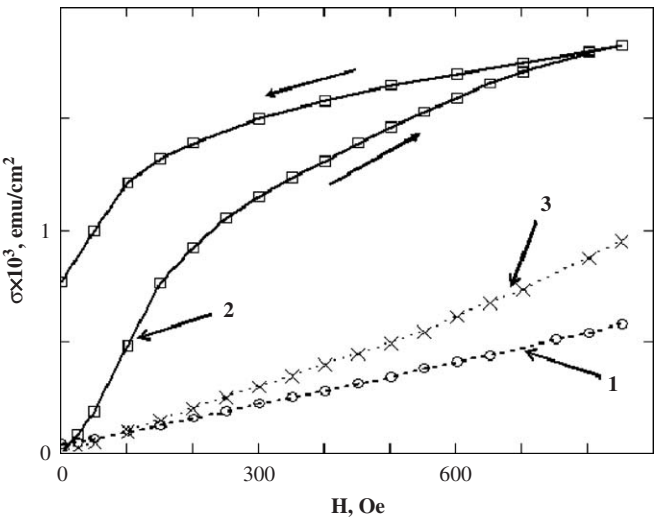

Fig. 4. Field dependence of magnetization in Co/Ge/Co films. Curve 1—$t_{Co} = 9$ nm, curve 2—$t_{Co} = 10.5$ nm, curve 3—$t_{Co} = 13.2$ nm, $T = 4.2$ K.

4. Discussion

Thus, the TEM and NMR data show that the all films made are heterophase, and the phase type, and its relative amount, are dependent on the thickness (or, actually, the volume) of the cobalt layer. In all the films, cobalt is present in its amorphous and/or cubic phases. All films have at least two phases with respect to the magnetization state of cobalt.

Earlier was shown that the state of the germanium is dependent on the germanium grain size. It is amorphous when the grain diameter d is $\leqslant 10$ nm (germanium layer thickness $t_{Ge} < 2.5$ nm), and is crystalline when $d \geqslant 50$ nm ($t_{Ge} > 5$ nm). When the grain diameter is between these limits a mixture of phases occurs. Near the germanium–cobalt interface, the system takes on the structure of the germanium grain. Away from the interface, where there are practically only cobalt–cobalt interactions, a more stable structure is adopted, that is, amorphous phase tends towards cubic phase [7]. As the cobalt layer thickness is increased, the cubic phase tends to transform to the hexagonal phase.

We recall that the cubic phase of polycrystalline cobalt is more easily magnetized than the amorphous and hexagonal phases [8]. In the latter two cases, the distribution of local axes of magnetization within the grains is chaotic, the local magnetic anisotropy is so strong that it is the determining factor in the magnetization. When the system is cooled at ZFC, a metastable state is created. It has been seen that $M(T)$, similar to those shown in Fig. 3 by the curves 1 and 3 or 4 and 6, occur when the cobalt grains are not dispersed but rather joined together [8]. Otherwise a cusp is not seen on the $M(T)$. Thus, it appears that the regions of different magnetic phases are exchange coupled. Since there is no magnetization in low fields up to 150 K, it follows that, here, either a negative exchange, or an energy barrier exists between the separate regions of different directions of magnetization. Otherwise the magnetization would increase immediately.

Thus, this model implies that an increase of the magnetic field at low temperatures already by itself orients the magnetic moment of certain parts of the films. This background magnetization surmounts the barrier associated with thermo-activation processes, thus giving rise to an increase in the total magnetization already at the lowest temperatures. The energy barrier might be due to the amorphous structure of cobalt part, or the dispersion of local anisotropy axes of the magnetic areas of cubic and hexagonal cobalt, or exchange anisotropy effects when some amount of exchange couplings are hindered. It is most likely, however, that a combination of these mechanisms occurs.

5. Conclusion

For fixed germanium layer thickness, the magnetization of a Co–Ge–Co system is dependent on the thickness of the ferromagnetic Co layers, and is related to the formation and distribution of the different magnetic phases, (HCP) and (FCC), of the cobalt. This result is directly relevant to the fabrication of real devices, where it is desirable to have a linear dependence of the magnetization on an external field.

Acknowledgements

The authors would like to thank G.V. Bondarenko for doing the X-ray measurements on films investigated. This research has been partly supported by Russian Foundation for Basic Research (Grant no 05-02-16671-a) and Federal Program of the University of Russia (Grant no UR-01.01.097). Also this work was supported by Grant no. RTI04-01-03 from the Regional Technology Innovation Program of the Ministry of Commerce, Industry and Energy (MOCIE) of Republic of Korea.

References

[1] S. Toscano, B. Briner, H. Hopster, M. Landolt, J. Mag. Mag. Mater 114 (1992) L6.
[2] B. Briner, M. Landolt, Phys. Rev. Lett. 73 (1994) 340.
[3] G.S. Patrin, N.V. Volkov, V.P. Kononov, Pis'ma Zh. Eksper. Teor. Fiz. 68 (1998) 287.
[4] G.S. Patrin, N.V. Volkov, S.G. Ovchinnikov, et al., Pis'ma Zh. Eksper. Teor. Fiz. 80 (2004) 560.
[5] P. Grunberg, J. Phys.: Condens. Matter. 13 (2001) 7691.
[6] X. Batlle, A. Labatra, J. Phys. D: Appl. Phys. 35 (2002) R15.
[7] E.P.Wohlfarth, Iron, Cobalt and Nickel. In: E.P.Wohlfarth (Ed.), Ferromagnetic materials, A Handbook on the Properties of Magnetically Ordered Substances, vol.1, North-Holland Publishing Company, Amsterdam, 1980, p.1.
[8] J.C. Denardin, M. Knobel, L.S. Dorneles, L.F. Schelp, J. Mag. Mag. Mater. 294 (2005) 206.